

Ionization of Al recoiled and sputtered from Al(100)X. Chen,¹ Z. Sroubek,^{1,2} and J. A. Yarmoff^{1,*}¹*Department of Physics, University of California, Riverside, California 92521, USA*²*Czech Academy of Sciences, URE, Chaberská 57, Prague 8, Czech Republic*

(Received 10 November 2004; revised manuscript received 28 February 2005; published 21 June 2005)

The absolute ionization probability of energetic (>500 eV) particles recoiled from Al(100) by 2 and 5 keV Xe⁺ bombardment was measured with time-of-flight spectroscopy. These values were then used to calibrate the energy and angular distributions of low-energy (10–600 eV) sputtered ions collected with an electrostatic analyzer. The independent-particle model of nonadiabatic surface-atom charge exchange, which is typically used to analyze single scattering events, was applied to the ion fractions of the recoiled and sputtered atoms. The model describes all the experimental data from a few eV to the keV range if a different surface electronic temperature is used for recoiling and sputtering. This suggests that the ionization process depends on the instantaneous surface condition at the time of ion emission.

DOI: 10.1103/PhysRevB.71.245412

PACS number(s): 68.49.Sf, 79.20.Rf, 68.47.De, 34.50.Dy

I. INTRODUCTION

The mechanism of ionization of atomic particles emitted from solids during sputtering by fast atomic projectiles is scientifically and technologically important, yet it is not fully understood. Despite many studies having been devoted to the subject,^{1–4} controversies still exist regarding the basic physical principles of the ionization process. This is in contrast to the related process of ionization (or neutralization) of particles scattered from a solid surface by a single binary collision, for which a remarkable success in identifying the factors governing charge formation has been achieved.^{5–9} It may be argued, however, that scattered and sputtered particles should be ionized by similar means because only outgoing trajectories of scattered particles are important in determining the charge state according to the well-documented memory-loss effect in the scattering of many kinds of ions. Up to now, however, a comparison of ionization in scattering and sputtering has not been achieved because of a lack of suitable experiments. In this paper, we present experimental data that allow such a comparison to be made over a wide range of secondary particle energies. The data provide a basis that can be used for further theoretical studies of surface electronic dynamics during secondary particle emission.

Aluminum was chosen for these studies for a number of reasons. It resembles an ideal metal and the basic theory can be precisely formulated only for jelliumlike substrates. Moreover, if the mechanism is a resonant charge-exchange process, the small gap between ionization energy of Al (5.98 eV) and the surface work function (4.4 eV) guarantees a sufficient yield of Al ions so that accurate experimental measurements of the absolute ionization probability can be made. In addition, the ionization potential of Al is close to that of Li, which enables the extrapolation of parameters from prior Li scattering experiments.⁷ Another advantage to the use of aluminum for these experiments is that the contribution of $2p$ deep hole excitations to the ionization of Al during sputtering is minimal, as revealed by the absence of any threshold effects in the dependence of Al⁺ formation on the energy of the bombarding particle. Thus, a resonance

ionization process involving only Al $3s$ and $3p$ electrons is the most probable mechanism.

Values of the ionization probability P^+ were obtained spanning the range of kinetic energies from hyperthermal up to kilovolts. Time-of-flight (TOF) spectroscopy was used to measure absolute values of P^+ in the range of 550–2000 eV for directly recoiled Al atoms generated by the impact of energetic Xe⁺ ions on atomically clean Al(100). Values of the ionization probability at lower energies were obtained by using the TOF data to calibrate prior work in which the relative behavior of P^+ for low-energy sputtered Al was measured in the range of 5–200 eV.¹⁰ To determine the ionization efficiency at even lower velocities, the angular dependence of the ion yield was measured for 10 eV Al⁺ ions sputtered by 2 keV Xe⁺.

The complete set of ionization probabilities was compared to a calculation based on the independent-particle nonadiabatic model,^{11,12} which has been successfully used in describing scattering data. The analysis shows that this simple model can reproduce the experimental data for both sputtered and recoiled Al, although a higher surface electronic temperature must be utilized for sputtered particles. The need to include a higher temperature for sputtered particles can be explained by considering the instantaneous state of the surface at the time of particle emission.

II. EXPERIMENTAL PROCEDURE

The experiments were carried out in an ultrahigh-vacuum chamber with a base pressure of 5×10^{-11} torr. The sample was mounted on a manipulator that allows for polar and azimuthal rotations. The Al(100) sample was cleaned by Ar⁺ sputtering, and then annealed to 470 °C using a resistive heater mounted beneath the sample holder. The surface order was checked with low-energy electron diffraction, and the surface cleanliness was verified with Auger electron spectroscopy. A Colutron ion source with a velocity (mass) filter produced a beam of Xe⁺ ions with a spot size of about 2 mm at the sample. The emitted particles were detected either by the TOF spectrometer, which can measure absolute values of

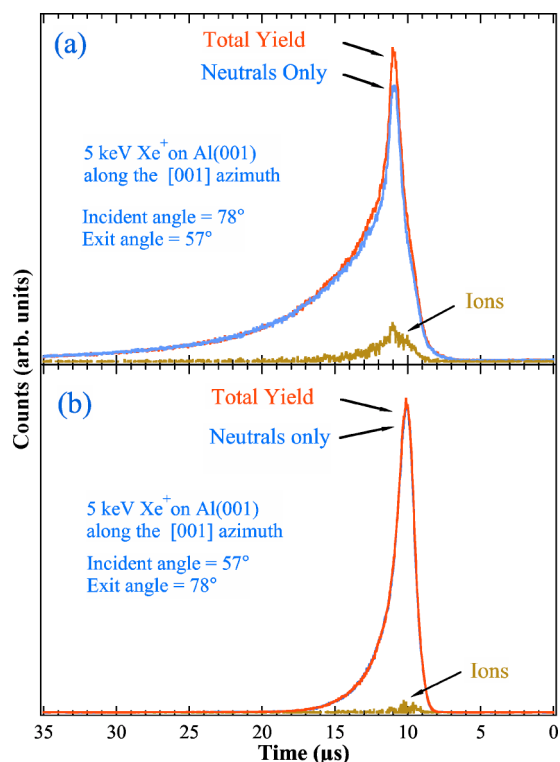


FIG. 1. (Color online) TOF spectra of energetic Al atoms recoiled from Al(100) by the impact of 5 keV Xe^+ ions. The exit angles are along the [001] azimuth and at (a) 57° and (b) 78° with respect to the surface normal.

P^+ ,⁷ or by a Comstock electrostatic analyzer (ESA), which detects only scattered ions. For TOF, the ion beam was pulsed at 20 kHz by rastering it across an aperture. The recoiled particles were measured by TOF at an angle of 135° with respect to the incident beam after traveling through a 1.09-m-long flight tube. Recoiled ions and neutrals were counted by a dual microchannelplate (MCP) array with the entrance held at ground potential to insure equal collection efficiency of ions and neutrals. A set of parallel deflection plates in the flight path is used to deflect the scattered ions when measuring the neutral yield by placing +250 V on one of the plates. The Comstock ESA is a 160° sector with a MCP detector operated in the constant pass energy mode. It is mounted on an adjustable turntable that allows for the selection of an arbitrary scattering angle.

III. RESULTS

Typical TOF spectra for 5 keV Xe^+ incident on Al(100) are shown in Fig. 1. The “Total Yield” and “Neutrals Only” curves display raw data, while the “Ions” curve shows the numerical difference. The data are plotted with respect to decreasing flight time, as shorter flight times correspond to higher particle velocity and therefore larger energy. The main peak at 10–12 μs consists entirely of recoiled Al, as was verified with Monte Carlo simulations using the code of Ref. 13. Although there may be a small contribution from scattered Xe at long flight times in the upper spectrum, it does

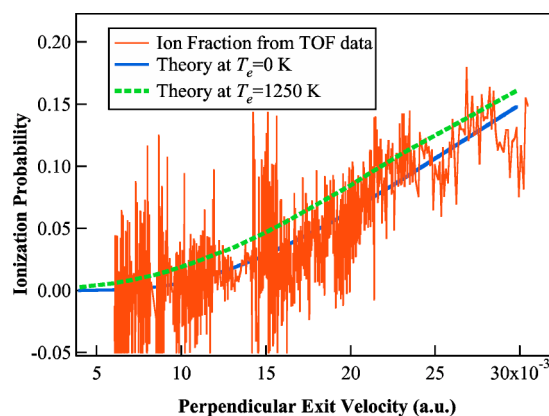


FIG. 2. (Color online) The ionization probability P^+ measured by TOF for Al atoms recoiled by 2 and 5 keV Xe^+ ions shown as a function of the perpendicular component of the Al exit velocity v_\perp . The calculated probability is shown by a solid line for $T_e=0$ K and by a dashed line for $T_e=1250$ K.

not interfere with the ionization yields measured for Al. In the lower spectrum, the contribution from Xe is negligible due to the particular scattering geometry.

The model used for resonant charge-transfer processes in scattering implies that the component of the exit velocity along the surface normal v_\perp is the important parameter in determining the ionization efficiency. A plot of P^+ as a function of v_\perp is thus the natural way in which to display the data, since the ionization of emitted particles depends only upon v_\perp in metals such as Al.^{5,7} v_\perp can be varied by changing the impact energy or by rotating the sample. Data collected at many different angles and for both 2 and 5 keV incident Xe^+ energies were used to determine the relationship between the ionization probability P^+ and v_\perp . Note that rotation changes both the initial Xe impact angle and the Al exit angle, as the scattering angle is fixed in our instrument. Although changing the impact angle can alter the energy distribution and yield of the emitted ions, this would not directly affect the ion fraction in a purely resonant process.

For each particular TOF spectrum, the ion yield spectrum was divided by the total yield spectrum to obtain values for the ionization probability P^+ over the time range that contained useful data. A segment of P^+ values versus flight time was thus determined around the center of the main peak for each spectrum collected at a different energy and angle. The measured flight times were then converted to the perpendicular component of the exit velocity v_\perp by assuming that all emitted species are ^{27}Al . To minimize errors due to small statistics at the sides of the main peak, the segments are cut off when the counts fall below typically 20% of the maximum intensity. Such segments of P^+ are compiled and plotted in Fig. 2 as a function of v_\perp . Note that Fig. 2 shows the raw data without any attempt at smoothing. It is seen that the ionization increases with velocity, as expected for a nonadiabatic resonant process.

Figure 3 shows how P^+ depends on changes to the surface work function, $\Delta\phi$, which was increased by deposition of iodine from a solid-state electrochemical cell.^{14,15} The ionization of Al P^+ increases rapidly with the work function.

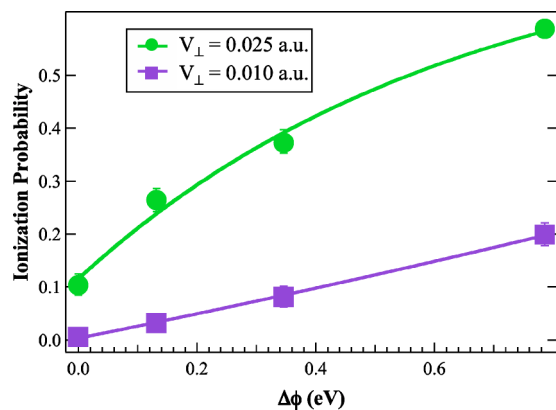


FIG. 3. (Color online) The ionization probability measured by TOF for Al atoms recoiled by 5 keV Xe⁺ shown vs iodine-induced work-function change for two values of v_{\perp} .

The increase goes as $\exp(\text{const } \Delta\phi)$ for the smaller v_{\perp} , and begins to saturate for the larger v_{\perp} . Although the deposition of iodine may induce a modification of the surface electronic structure, which cannot be entirely described in terms of the general work function,^{14,15} the net result is qualitatively consistent with a nonadiabatic resonant ionization process.

Thus, the raw data in both Figs. 2 and 3 support the notion that ionization of the emitted Al is determined by a resonant charge-transfer mechanism. Although such processes are reasonably well understood for alkali-metal systems, ionization for metal-metal systems has not been extensively investigated because of the difficulty in preparing metal ions for scattering, and also because the difference between the ionization potential and the work function of most metals is usually large enough that few ions are produced. The use of TOF to investigate fast recoiled Al obviates both of these difficulties for energies above a few hundred eV.

Values of the ionization probability for energies below those accessible with TOF were obtained from prior work in which the relative behavior of P^+ for low-energy sputtered Al was measured by Garrett *et al.*¹⁰ in the range of 5–200 eV using an ESA. Values of P^+ for energies up to 600 eV were obtained from these data by extrapolation using the empirical formula $P^+ \propto (v_{\perp})^{2.2}$ derived in Ref. 10. The squares in Fig. 4 show the measured P^+ of Al emitted along the surface normal by sputtering, taken from Ref. 10. The data were calibrated to our absolute TOF measurements at 600 eV so that the vertical scale in Fig. 4 provides the absolute ionization probability.

It should be mentioned that the ionization of sputtered Al has been experimentally studied by several authors, but the work in Ref. 10 seems to be one of the most complete for the purpose of a comparison with recoiled ions. In a more recent experimental study of P^+ for Al,¹⁶ the relative values above 80 eV were empirically fit by the exponential relationship $P^+ \propto \exp(-v_0/v_{\perp})$, where $v_0 = 8 \times 10^6$ cm/s. In the range from 80 to 600 eV, however, this exponential dependence cannot be experimentally distinguished from the power law suggested in Ref. 10 and used in our analysis. It should be stressed that in both Refs. 10 and 16 only relative values of P^+ could be measured, and this is not sufficient for the comparison with theoretical predictions.

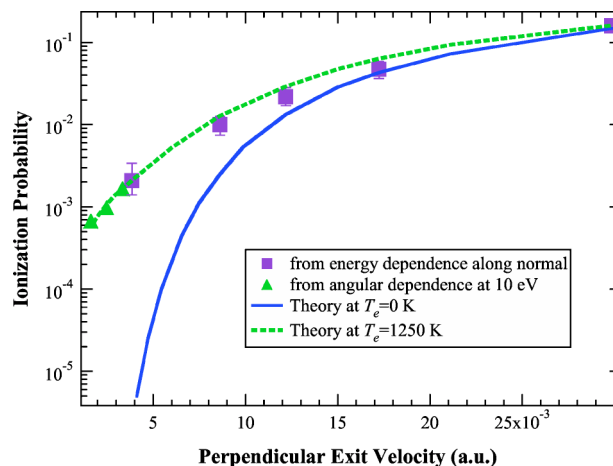


FIG. 4. (Color online) The ionization probability P^+ of sputtered Al shown as a function of the perpendicular component of the exit velocity v_{\perp} . The squares were taken from Ref. 10 and calibrated by our TOF data, and the triangles are from our measurements. The values of P^+ calculated from Eq. (1) are shown by a solid line for $T_e=0$ and by a dashed line for $T_e=1250$ K.

The angular dependence of the ion yield for 10 eV Al⁺ ions sputtered from Al(100) was used to determine the ionization efficiency at even lower velocities. Note that this energy is still high enough that it avoids possible complications due to the image charge effect. The resonance model used to analyze the data suggests that ionization of 10 eV Al atoms occurs far away from the surface, which reduces the image charge potential to less than 0.8 eV.

The triangles in Fig. 4 show how P^+ changes with exit angle for 10 eV Al, as measured in our setup. The sample was bombarded by 2 keV Xe⁺ at an impact angle of 30°, and Al⁺ ions were measured with the ESA as the turntable was rotated to vary the exit angle. Because of the cosine angular dependence of the flux of sputtered particles, the measured ion current was divided by $\cos \theta$ (where θ is the angle with the respect to the surface normal) to obtain relative values of P^+ . The value of P^+ was normalized at $\theta=0^\circ$ to P^+ at 10 eV obtained from the normalized data of Ref. 10. It should be mentioned that the ion fractions at and below 10 eV ($v_{\perp}=3.8 \times 10^{-3}$ a.u.), where most of the sputtered particles are emitted, have also been independently estimated in dynamically cleaned samples by secondary ion mass spectroscopy (SIMS) techniques¹⁷ to be 1.1×10^{-3} , in a close agreement with our results.

IV. DISCUSSION

To interpret the data on Al⁺ ionization, we use the standard formulation of the problem in terms of the Anderson-Newns dynamical Hamiltonian (e.g., see Ref. 18). The most appropriate solution of the Hamiltonian would be in terms of the multiple many-body configuration approach,¹⁸ which includes the spin-orbital degeneracy of Al 3p in a natural fashion. This model becomes too complex, however, for systems with more electrons, and a limited number of configurations must be carefully chosen to make it

solvable. So, for the present data, we resort to the simpler independent-particle model in its integral form,^{5,11,12} which has been widely used to describe electronic processes in low-energy ion scattering, i.e.,

$$P^+ = \frac{1}{\pi} \int d\varepsilon [1 - f(\varepsilon, T_e)] \left| \int_{-\infty}^{+\infty} \left(\frac{\Delta(t')}{2} \right)^{1/2} \times \exp \left[-i\varepsilon t' - \int_{t'}^{\infty} \left(i\delta(t'') + \frac{\Delta(t'')}{2} \right) dt'' \right] dt' \right|^2, \quad (1)$$

where $f(\varepsilon, T_e)$ is the Fermi distribution with the Fermi energy set to zero. This model describes charge exchange during scattering quite well in terms of a few parameters that can be reasonably estimated from the actual physical situation. The parameters are the difference δ between the substrate work function and the ionization energy of the emitted atom, the virtual linewidth Δ of the ionization level, the component of the exit velocity along the surface normal v_{\perp} , and the electronic temperature T_e of the substrate. In the spirit of the independent-particle model, the Fermi distribution $f(\varepsilon_f, T_e)$ does not take into account the degeneracy of the Al ionization level, and the Al $3p$ levels are substituted by one nondegenerate level. Both δ and Δ are functions of the distance z of the emitted Al atom from the surface and thus they are functions of time, as $z = v_{\perp} t$. The z dependence is caused by the image charge effect and by charge exchange with the surface. For Al atoms interacting with Al metal, the following expressions for δ and Δ were used (in a.u.):

$$\delta(z) = -0.058 + (16z^2 + 109.44)^{-1/2}, \quad (2)$$

$$\Delta(z) = 1.5[\exp(3.316z) + 332523]^{-1/4}. \quad (3)$$

Relation (2) is the commonly used expression for the image charge effect, which takes into account the actual values of the Al ionization energy (5.98 eV) and the Al work function (4.4 eV) and saturates close to the surface. The distance $z=0$ corresponds to the surface passing through the center of the outermost layer of surface atoms. It defines the boundary of the jellium substrate and is assumed to coincide with the image reference plane. Equation (3) was taken from Ref. 5, and accounts for both the exponential decrease of $\Delta(z)$ away from the surface and for the saturation close to it. As the saturation value of Δ and the decay constant γ have not yet been calculated for the Al-Al metal system, values calculated for the Li-jellium system were used in Eq. (3), i.e., $\gamma=0.83$ a.u.⁻¹ and $\Delta=1.7$ eV.¹⁹ The width of the Al ionization level is not expected to be very different from the width of the Li level, as both have similar ionization energies. The ionization probability (P^+) of Al, obtained from Eq. (1) using Eqs. (2) and (3) with $T_e=0$, is plotted as a solid line in Fig. 2 along with the experimental data.

The good quantitative agreement between the theory and the experiment in Fig. 2 indicates that the high-energy recoiled ions are indeed formed by a nonadiabatic process and that the formation is well described by Eq. (1) with the substrate at $T_e=0$. The agreement also proves the applicability of Eq. (1) for purely metallic systems where the particle is completely neutral prior to emission (in contrast to typical

scattering experiments with alkali ions) and contains more valence electrons.

The situation changes dramatically, however, if the same relation is used to describe the ionization of sputtered Al at lower kinetic energies. The disagreement is clearly apparent in Fig. 4 where P^+ , calculated from Eq. (1), is plotted by a solid line for $T_e=0$. Whereas the calculated P^+ agrees well with the experiment above about $v_{\perp}=20 \times 10^{-3}$ a.u., it is smaller by two orders of magnitude at $v_{\perp}=5 \times 10^{-3}$ a.u. The predicted dependence is not only much steeper than the experimental data but it is also too small by factor of 1000 at the lowest velocities. This large discrepancy at low velocities cannot be reduced by any other choice of Δ and γ .

The theory and the experimental ionization probabilities for sputtered particles can be put into agreement, however, if T_e in Eq. (1) is not zero but is instead set equal to 1250 K in the one-electron scheme and with our choice of $\Delta(z)$. The values of P^+ calculated from Eq. (1) using $T_e=1250$ K while keeping the other parameters the same are shown in Fig. 4 by the dashed line. The values of P^+ above a kinetic energy of 200 eV ($v_{\perp} \sim 17 \times 10^{-3}$ a.u.) are only very slightly influenced by the introduction of a nonzero T_e , but the values of P^+ are increased considerably at lower energies. The agreement between the theory and experiment is very good for both the energy dependence and the angular dependence of P^+ over the entire range. The quantitative fit of Eq. (1) to the angular dependence of low-energy sputtered Al⁺ ions indicates that the surface of the Al metal is well defined even in the collision cascade. Our preliminary estimates indicate that by decreasing γ in Eq. (3), which seems to be appropriate for the more spread-out Al $3p$ level, and by taking into account the spin-orbital degeneracy of the Al ground state, a similarly good agreement with the experiment can be obtained with still higher T_e .

In contrast to sputtering, a high value of T_e is not needed to describe fast particles in scattering and recoiling. The calculation of P^+ from Eq. (1) with $T_e=1250$ K is shown in Fig. 2 along with the data for recoiled Al. It is clear that the experimental data more closely follow the theory with $T_e=0$ K than with $T_e=1250$ K. In addition, experiments have shown that for scattered hyperthermal alkali ions within the same low-energy range,²⁰ the fully quantal expression (1) is valid with $T_e=0$ even at energies below 10 eV.

These results indicate that the high value of T_e invoked for sputtered particles is characteristic of dynamically perturbed surfaces in the collision cascade region. It is not clear from the data, however, whether T_e is a real temperature of the electron gas in the substrate or a parameter that heuristically describes a smearing of the Fermi level by local collision-induced perturbations. It has been shown for the case of Na (Ref. 20) and calculated for Al (Ref. 21) that such perturbations can affect charge exchange via collision-induced changes in the electrostatic potential near the surface. The induced changes of the potential are relatively small (a few tenths of an eV) and of a short range and may not influence the ionization of Al atoms, which are substantially more difficult to ionize than Na. On the other hand, the concept of T_e as the temperature of the electronic system, produced in the cascade by moving substrate atoms, seems to be substantiated by the very good agreement with the experiment in Fig. 4.

High electronic temperatures have been invoked^{22,23} and studied in detail^{2,24} in order to account for the large, not previously explained ion yields observed in the sputtering of Cu, Nb, and Ta metals. In this paper, we have extended these studies by determining T_e quantitatively in Al for which the other surface charge-exchange parameters were obtained independently from recoil and scattering experiments. By using Al as the substrate, we also avoid ambiguities due to the possible contribution of d -hole excitations to P^+ in heavier metals. The relative simplicity of the Al system may help to clarify the precise physical content of the parameter T_e , in particular whether T_e is a parameter characterizing the smearing of the Fermi energy by electrostatic potentials in an inhomogeneous electron gas or whether T_e is the actual temperature of electron-hole pairs dynamically created in the cascade. If T_e is the temperature of electron-hole pairs in a broad Al s - p band, a considerable confinement of electronic excitations within the cascade region is needed to obtain such high electronic temperatures.³ The mechanism of confinement has not yet been fully determined. It is conceivable that the high degree of temporary amorphization and electronic excitation in the cascade avoids a rapid dissipation of the excitation by a drastic shortening of the electron mean free path, as discussed in detail in Ref. 25.

V. CONCLUSIONS

It has been shown that ionization in scattering, recoiling, and sputtering can be described by the same type of resonant charge-transfer process. In all cases, the charge state is determined along the exit trajectory, and reflects the alignment of the surface potential with the ionization level of the exiting atomic particle. There is a critical difference, however, in the application of this analysis to sputtered, as opposed to scattered and recoiled, particles. The former are emitted from a surface perturbed by a collision cascade, while the latter exit from the solid before any perturbation has occurred. The effects of the perturbation can be modeled by increasing the surface electronic temperature in the nonadiabatic independent-particle model. Thus, any complete theory of charge exchange must consider the instantaneous state of the surface at the time of particle emission.

ACKNOWLEDGMENTS

The authors are indebted to Dr. J. Lorincik, Professor A. Wucher, and Professor P. Williams for helpful discussions. This work was supported by the National Science Foundation (Grant No. CHE-0091328) and the Czech Academy of Sciences (Grant No. A1067401).

*Corresponding author. FAX 951-827-4529; Email address: yarmoff@ucr.edu

¹S. F. Belykh, V. V. Palitsin, A. Adriaens, and F. Adams, Nucl. Instrum. Methods Phys. Res. B **203**, 172 (2003).

²D. V. Klushin, M. Y. Gusev, S. A. Lysenko, and I. F. Urazgil'din, Phys. Rev. B **54**, 7062 (1996).

³Z. Sroubek and J. Lorincik, Surf. Rev. Lett. **6**, 257 (1999).

⁴M. L. Yu, *Sputtering by Particle Bombardment III* (Springer, Berlin, 1991).

⁵G. A. Kimmel and B. H. Cooper, Phys. Rev. B **48**, 12 164 (1993).

⁶C. E. Sosolik, J. R. Hampton, A. C. Lavery, B. H. Cooper, and J. B. Marston, Phys. Rev. Lett. **90**, 013201 (2003).

⁷C. B. Weare and J. A. Yarmoff, Surf. Sci. **348**, 359 (1996).

⁸K. Niedfeldt, E. A. Carter, and P. Nordlander, J. Chem. Phys. **121**, 3751 (2004).

⁹J. P. Gauyacq and A. G. Borisov, J. Phys.: Condens. Matter **10**, 6585 (1998).

¹⁰R. F. Garrett, R. J. MacDonald, and D. J. O'Connor, Surf. Sci. **138**, 432 (1984).

¹¹W. Bloss and D. Hone, Surf. Sci. **72**, 277 (1978).

¹²R. Brako and D. M. News, Surf. Sci. **108**, 253 (1981).

¹³V. Bykov, C. Kim, M. M. Sung, K. J. Boyd, S. S. Todorov, and J. W. Rabalais, Nucl. Instrum. Methods Phys. Res. B **114**, 371 (1996).

¹⁴Y. Yang, Z. Sroubek, and J. A. Yarmoff, Phys. Rev. B **69**, 045420 (2004).

¹⁵J. A. Yarmoff, Y. Yang, and Z. Sroubek, Phys. Rev. Lett. **91**, 086104 (2003).

¹⁶A. Tolstogousov, S. F. Belykh, M. Stepnova, S. K. Dew, and C. Pagura, Surf. Rev. Lett. **11**, 391 (2004).

¹⁷J. Lorincik, P. Williams, and K. Franzreb (personal communication).

¹⁸J. B. Marston, D. R. Andersson, E. R. Behringer, B. H. Cooper, C. A. DiRubio, G. A. Kimmel, and C. Richardson, Phys. Rev. B **48**, 7809 (1993).

¹⁹E. R. Behringer, D. R. Andersson, B. H. Cooper, and J. B. Marston, Phys. Rev. B **54**, 14 765 (1996).

²⁰C. A. Keller, C. A. DiRubio, G. A. Kimmel, and B. H. Cooper, Phys. Rev. Lett. **75**, 1654 (1995).

²¹J. A. M. C. Silva, J. Wolfgang, A. G. Borisov, J. P. Gauyacq, P. Nordlander, and D. Teillet-Billy, Nucl. Instrum. Methods Phys. Res. B **157**, 55 (1999).

²²Z. Sroubek, Phys. Rev. B **25**, 6046 (1982).

²³Z. Sroubek, Spectrochim. Acta, Part B **44**, 317 (1989).

²⁴D. V. Klushin, M. Y. Gusev, and I. F. Urazgil'din, Nucl. Instrum. Methods Phys. Res. B **100**, 316 (1995).

²⁵A. Duvenbeck, F. Sroubek, Z. Sroubek, and A. Wucher, Nucl. Instrum. Methods Phys. Res. B **225**, 464 (2004).